

Polarization effect on optical manipulation in a three-beam optical lattice

Guangji Ha, Hongxia Zheng, Xinning Yu,^{*} and Zhifang Lin[†]

State Key Laboratory of Surface Physics and Department of Physics, Fudan University, Shanghai 200433, China



(Received 19 May 2019; published 12 September 2019)

We study the effect of polarization on optical micromanipulation in a hexagonal optical lattice formed by three equiamplitude plane waves that have their wave vectors lying equiangularly in a plane, taking into account the vectorial characteristic of the electromagnetic waves. It is demonstrated that different polarizations generate different optical force landscapes, resulting in a trapping versus detrapping phenomenon tunable by tailoring the polarization of the incident beams. The physical origin of the polarization effect on the force landscapes is then traced to the ratio between the conservative (gradient) and nonconservative (scattering) optical forces acting on a particle immersed in the three-wave optical lattice. The trapping-detrapping transition phenomenon due to the change of polarization in small particles, where the gradient force dominates, is revealed to originate from the reverse of the conservative optical force, which manifests itself by a transition of the optical potential energy landscape from one exhibiting a periodic distribution of pits to one showing a distribution of humps over space. Our results suggest an alternative handle to manipulate small particle by tuning the polarization.

DOI: [10.1103/PhysRevA.100.033817](https://doi.org/10.1103/PhysRevA.100.033817)

I. INTRODUCTION

Light transfers momentum to an object in the way of its propagation and exerts a force on the latter along the propagation direction. This is known as the radiation pressure. The concept of radiation pressure was confirmed by the classical theory of electromagnetism [1], which laid the solid theoretical foundation for further investigation of the optical force. The successful experimental trapping of microparticles by employing two laser beams was first realized in [2]. Later on, the optical trapping of a dielectric particle by a single highly focused laser beam was implemented experimentally in [3]. The single-beam optical trappings, known later as optical tweezers [4], have been applied to a variety of objects ranging in size from cells to atoms [5], rated among the most recognized applications of the optical force.

The technique of noncontact optical manipulation, including optical trapping, accelerating, transporting, and even pulling, has been extensively investigated in a variety of areas [4–19]. The target of optical manipulation is not limited to a single particle, but includes multiple particles as well. To achieve multiparticle manipulation, one can employ the optical field composed of interfering beams to produce periodic arrays of trapping sites [20–25], enabling particles to be trapped in these sites and forming optical matter, provided particles are small enough so that the interaction stemming from multiple scattering can be ignored. Thus, the investigation of the optical trapping of a particle in a periodic optical field, termed the optical lattice, can be considered as a pathfinder for constructing optical matter made up of multiple particles.

In this paper we study the optical force field acting on a particle immersed in a simple three-beam optical lattice

that is formed by three identical (with the same polarization and amplitude) plane waves with their wave vectors lying equiangularly in a plane, namely, the angle between any two wave vectors is 120° . We focus on how the polarization of the incident plane waves affects the force landscape and yields different physical consequences in optical manipulation, taking into consideration the vectorial characteristic of the optical field. Using the above configurations, previous works have reported the particles of a dipole ($r \ll \lambda$) [25]. Meanwhile, the particles in the ray optics regime ($r \gg \lambda$) were theoretically and experimentally studied by Hou *et al.* [26]. However, Mie particles ($r \approx \lambda$), which are commonly used in experiments, have not been studied due to the region beyond the dipole approximation and ray optics approximation. Following the work of Ng and co-workers [27,28], we rigorously decompose the total optical force exerted on spherical particles of arbitrary size into the gradient and scattering forces in the three-beam optical lattice and study the polarization effects of the dipole and Mie particles. We demonstrate that the polarization effect in the simple three-beam optical lattice owes its physical origin to the ratio between these two force components. Our results thus suggest an alternative way of optical manipulation of a microparticle by tailoring the polarization. A typical example is given in which one can tune the optical potential energy landscape from a periodic distribution of pits to a distribution of humps, leading to a transition from trapping to detrapping through modulating the polarization of the constituent beams of the optical lattice.

II. RESULTS AND DISCUSSION

The electric field of the simple three-beam optical lattice is given by

$$\mathbf{E}(\mathbf{r}, t) = \mathbf{E}_1(\mathbf{r}, t) + \mathbf{E}_2(\mathbf{r}, t) + \mathbf{E}_3(\mathbf{r}, t),$$

$$\mathbf{E}_j(\mathbf{r}, t) = E_0(p\hat{\theta}_{k_j} + q\hat{\phi}_{k_j})e^{i\mathbf{k}_j \cdot \mathbf{r} - i\omega t}, \quad j = 1, 2, 3, \quad (1)$$

^{*}15110190043@fudan.edu.cn

[†]phlin@fudan.edu.cn

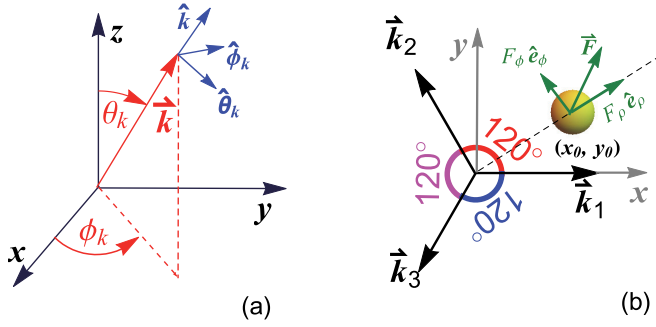


FIG. 1. (a) Schematic illustration of the coordinate system, where \hat{k} , $\hat{\theta}$, and $\hat{\phi}$ represent the direction of wave propagation and the directions of increasing polar angle and azimuthal angle, respectively. (b) Schematic plot of three wave vectors lying in the x - y plane for the three-beam optical lattice. The angle between any two of the wave vectors is 120° . A particle is immersed in the optical field with its center located at (x_0, y_0) . The optical force acting on the particle is written as $\mathbf{F} = F_\rho \hat{e}_\rho + F_\phi \hat{e}_\phi$ for stability analysis.

where $\hat{\theta}_k$, $\hat{\phi}_k$, and \hat{k} are the unit vectors in the spherical coordinate system [see Fig. 1(a)], ω and k represent the circular frequency and wave number in the background medium, respectively, and \hat{k} denotes the direction of the wave vector $\mathbf{k} = k\hat{k}$. In our case, the three wave vectors are all lying in the x - y plane, with the angle between any two of them being 120° , as shown in Fig. 1(b), to form a regular three-beam optical lattice. To be specific, the three wave vectors are given by

$$\mathbf{k}_1 = \hat{e}_x, \quad \mathbf{k}_2 = -\frac{1}{2}\hat{e}_x + \frac{\sqrt{3}}{2}\hat{e}_y, \quad \mathbf{k}_3 = -\frac{1}{2}\hat{e}_x - \frac{\sqrt{3}}{2}\hat{e}_y, \quad (2)$$

where \hat{e}_x and \hat{e}_y are two basis unit vectors in the Cartesian coordinates. Two complex numbers p and q characterize the polarization of each constituent plane wave making up the three-beam optical lattice. They constitute a two-dimensional complex vector (p, q) known as a polarization vector, with, e.g., $(p, q) = (1, 0)$ and $(0, 1)$ representing the linear polarization and $(p, q) = (1, i)$ corresponding to the left circular polarization [29]. Throughout this paper, the polarization vector (p, q) is normalized by $|p|^2 + |q|^2 = 1$ in all numerical calculations. We note that the three waves share the same amplitude $E_0 > 0$ and polarization (p, q) . The incident wavelength in the calculation is fixed to $\lambda = 720$ nm and the spherical particle is suspended in vacuum. The optical forces shown in any figure are in units of $\varepsilon_0 E_0^2 / k^2$. We will focus on the effect of the polarization denoted by (p, q) , while some previous studies [25] simply set the electric field to be along z , namely, perpendicular to the plane formed by three wave vectors and limited to the case with $(p, q) = (1, 0)$ in our notation.

The time-averaged optical force \mathbf{F} exerted on a particle by the optical field is computed based on the Maxwell stress tensor method [29–31] as well as the generalized Lorenz-Mie theory [32]. Due to the translational invariance of the system along z , we limit ourselves to the study of an optical force parallel to the wave-vector plane and present the force landscapes in the x - y plane. Figure 2 shows the landscapes of the radial component F_ρ of the optical force [see Fig. 1(b)

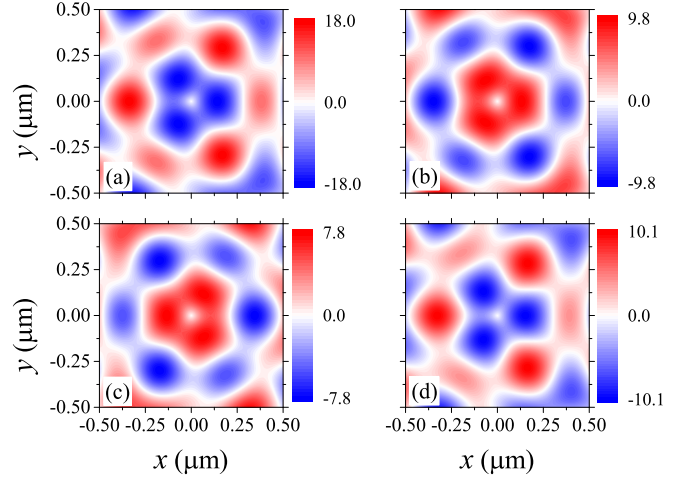


FIG. 2. Spatial profiles of the radial component of the optical force F_ρ on a gold particle with (a) and (b) $r = 0.1 \mu\text{m}$ and (c) and (d) $r = 0.31 \mu\text{m}$, immersed in the simple three-beam optical lattice. The left and right panels correspond to different polarization with (a) and (c) $(p, q) = (1, 0)$ and (b) and (d) $(p, q) = (0, 1)$. The results demonstrate transitions between trapping and detraping induced by polarization.

for a schematic illustration] exerted on a gold particle of radii $r = 0.1$ and $0.31 \mu\text{m}$, which correspond to dipole and Mie particles, respectively. The permittivity of gold refers to the Drude fit of experimental results and is set as $\varepsilon = -17.46 + 1.08i$ [33,34]. Each point in the force landscape displayed in Fig. 2 denotes the value of F_ρ acting on the particle centered therein. It is obvious that for a conventional optical lattice with the electric field polarized along z that circumvents the vectorial property of the electromagnetic field (corresponding to $q = 0$), a small gold particle can be trapped stably at the origin of the coordinate system [25] [see Fig. 2(a)] since the trapped particle will return to its equilibrium when displaced slightly, subject to the negative radial force. The trapping of multiple particles can therefore be expected from the periodicity of the optical lattice. However, when one changes the polarization to $p = 0$, with the electric field lying within the wave-vector plane, Fig. 2(b) implies that the trapping becomes unstable due to a sign change in the radial force. When a particle is displaced slightly from the equilibrium, it will be pushed farther away by the positive radial force. One may intuitively imagine that the vectorial character of light is unfavorable to the trapping, as observed from Figs. 2(a) and 2(b). The situation turns out being quite different when the particle size is increased. In Figs. 2(c) and 2(d) we show the radial force landscapes for a $0.31\text{-}\mu\text{m}$ -radius gold particle. Comparing Fig. 2(c) with Fig. 2(a), it is remarkable to find that aligning the electric field to z to avoid the vectorial property of light is not always favorable to the optical trapping. Tuning the polarization to make the electric field polarize within the wave-vector plane, where the vectorial property of the field comes into play, favors the trapping, as visualized in Fig. 2(d). One therefore concludes that the polarization will surely change the spatial distribution of the optical force, leading to a diversity of force landscapes and resulting in a trapping to detraping transition. As a result, one can manipulate the

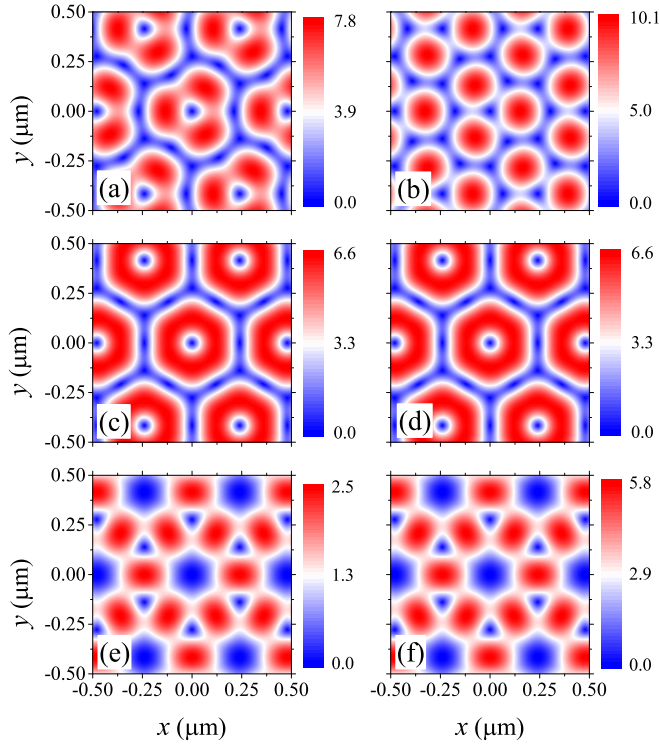


FIG. 3. Spatial profiles for the magnitudes of (a) and (b) total optical forces \mathbf{F} , (c) and (d) gradient forces \mathbf{F}_g , and (e) and (f) scattering forces \mathbf{F}_s acting on a gold particle with radius $r = 0.31 \mu\text{m}$ immersed in the three-beam optical lattice with different polarizations. The polarization vectors are (a), (c), and (e) $(p, q) = (1, 0)$ and (b), (d), and (f) $(p, q) = (0, 1)$. The diversity of optical force landscapes shown in (a) and (b) is caused by the change of relative magnitude in the gradient and scattering forces, which keep their spatial profiles unchanged with respect to different polarizations, as displayed in (c)–(f).

particle state such as from stable trapping to transporting, and vice versa, by modulating the polarization, taking full advantage of the vectorial feature of the light field.

To trace the physical origin of the polarization effect, following Ng and co-workers [27,28,35], we decompose the time-averaged optical force into the gradient and scattering parts \mathbf{F}_g and \mathbf{F}_s , respectively, given by

$$\begin{aligned} \mathbf{F} &= \mathbf{F}_g + \mathbf{F}_s, \\ \mathbf{F}_g &= -\nabla\varphi, \quad \mathbf{F}_s = \nabla \times \boldsymbol{\psi}, \end{aligned} \quad (3)$$

where φ and $\boldsymbol{\psi}$ are the potential energy and vector potential, respectively. Therefore, \mathbf{F}_g and \mathbf{F}_s correspond to the conservative and nonconservative forces [36], respectively. The landscapes for both the gradient and scattering forces, together with the total optical force \mathbf{F} , are illustrated in Fig. 3 for a $0.31\text{-}\mu\text{m}$ -radius gold particle. It can be observed that the spatial profiles for either the gradient or scattering do not change in the three-beam optical lattice, except for the magnitude, in agreement with the findings by Jiang *et al.* [35], as displayed in Figs. 3(c)–3(f). The change of optical force landscapes, as visualized in Figs. 3(a) and 3(b), arises from the relative magnitude of the conservative and nonconservative components. The invariance in the spatial profile is hidden

with the conservative and nonconservative components [35]. The change of the polarization modifies the distribution of the electric and magnetic fields over space, giving rise to the variation in the magnitudes of the conservative and nonconservative forces and thus bringing about a variety of polarization-dependent optical force landscapes as shown in Figs. 3(a) and 3(b).

The physics manifests itself further by an analytical expression [35] for the optical force exerted on a spherical particle of arbitrary size residing in the three-beam optical lattice described by Eqs. (1) and (2). It is derived that [35]

$$\begin{aligned} \mathbf{F}_g &= A\nabla|\mathbf{E}|^2 + C\nabla|\mathbf{B}|^2, \\ \mathbf{F}_{s\parallel} &= (D|p|^2 + G)\text{Re}(\mathbf{E} \times \mathbf{B}^*)_{\parallel}, \end{aligned} \quad (4)$$

where the real parameters A , C , D , and G , carrying appropriate physical units, show a very complicated dependence on the Mie coefficients [37], but they are independent of the polarization vector (p, q) [35]. The subscript \parallel denotes the in-plane (perpendicular to z) components of the scattering force. The gradient of the electric field intensity depends on the polarization through

$$\begin{aligned} \nabla|\mathbf{E}|^2 &= 3(1 - 3|p|^2) \cos \frac{\sqrt{3}\eta}{2} \sin \frac{3\xi}{2} \hat{\mathbf{e}}_x \\ &+ \sqrt{3}(1 - 3|p|^2) \left(\cos \frac{3\xi}{2} + 2 \cos \frac{\sqrt{3}\eta}{2} \right) \sin \frac{\sqrt{3}\eta}{2} \hat{\mathbf{e}}_y, \end{aligned} \quad (5)$$

where ξ and η are reduced Cartesian coordinates, given by $\xi = kx$ and $\eta = ky$. The gradient $\nabla|\mathbf{B}|^2$ of the magnetic field is obtained by replacing p with q in Eq. (5), due to electromagnetic duality. The in-plane time-averaged Poynting vector $\frac{1}{2}\text{Re}(\mathbf{E} \times \mathbf{B}^*)_{\parallel}$ is independent of the polarization, reading

$$\begin{aligned} \text{Re}(\mathbf{E} \times \mathbf{B}^*)_{\parallel} &= \left(\cos \frac{3\xi}{2} \cos \frac{\sqrt{3}\eta}{2} - \cos \sqrt{3}\eta \right) \hat{\mathbf{e}}_x \\ &+ \sqrt{3} \sin \frac{3\xi}{2} \sin \frac{\sqrt{3}\eta}{2} \hat{\mathbf{e}}_y. \end{aligned} \quad (6)$$

Equations (4)–(6) suggest the possibility of tuning the relative magnitude between the gradient and scattering forces by changing the polarization, yielding a diversity of force landscapes that affects the optical trapping and manipulation. In addition, the dependence on the Mie coefficients of the parameters A , C , D , and G allows for the manipulation of particles with different sizes by different polarizations, as illustrated in Fig. 2, where trapping of a $0.31\text{-}\mu\text{m}$ gold particle requires the electric field to be polarized in the wave-vector plane (normal to z) while trapping of $0.1\text{-}\mu\text{m}$ particle needs the electric field polarized along z , as a typical manifestation of the polarization effect on the optical trapping.

The trapping to detraping transition by tailoring the polarization is not limited to metallic particles only. It works on dielectric particles as well, even in the case where the gradient force is kept dominant when the polarization is modulated. It is well known, based on the optical Earnshaw theorem [38,39], that the scattering force will not trap any particle, since it satisfies $\nabla \cdot \mathbf{F}_s = 0$, violating the necessary condition of stable equilibrium $\nabla \cdot \mathbf{F} < 0$. One usually resorts to the

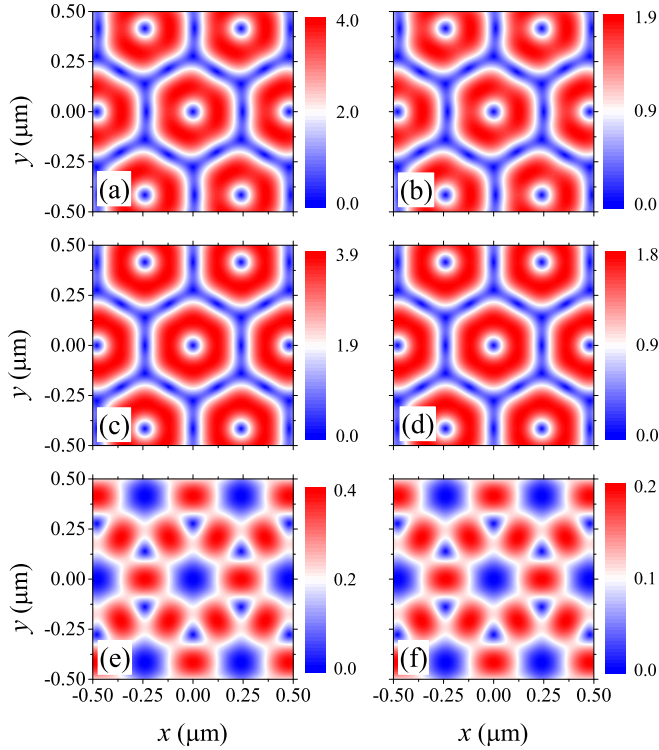


FIG. 4. Spatial profiles for the magnitudes of (a) and (b) total force \mathbf{F} , (c) and (d) gradient force \mathbf{F}_g , and (e) and (f) scattering force \mathbf{F}_s , acting on a polystyrene particle ($\varepsilon = 2.53$) with $r = 0.1 \mu\text{m}$ immersed in the three-beam optical lattice given by Eqs. (1) and (2). The left and right panels correspond to the polarization with (a), (c), and (e) $(p, q) = (1, 0)$ and (b), (d), and (f) $(p, q) = (0, 1)$. In both cases the gradient force far outweighs the scattering force.

gradient force for trapping. However, the dominant gradient force by no means implies a stable trapping. This is shown in Figs. 4, 5(a), and 5(b) for a polystyrene particle of radius $0.1 \mu\text{m}$. In both cases with the polarization $(p, q) = (1, 0)$

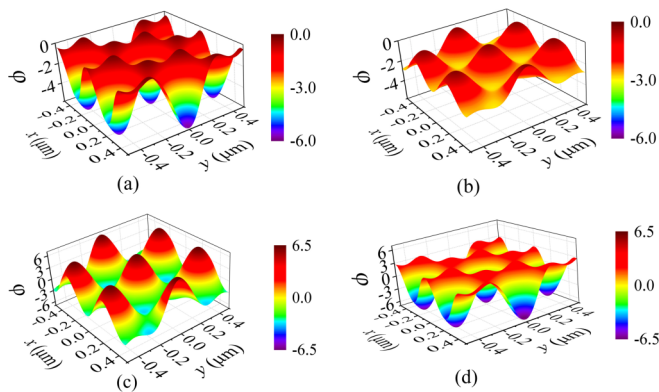


FIG. 5. (a) and (b) Potential energy ϕ landscapes corresponding to Figs. 4(c) and 4(d), visualizing the trapping and detraping phenomena due to the change of polarization. (c) and (d) Potential energy landscapes corresponding to Figs. 2(c) and 2(d). Although the scattering force is comparable to the gradient force, the potential energy landscape demonstrates the physical origin of a detraping to trapping transition induced by the polarization.

and $(p, q) = (0, 1)$ corresponding, respectively, to the electric field polarized along z and perpendicular to z in the three-beam optical lattice, the gradient force is nearly tenfold the magnitude outweighing its counterpart, the scattering force. The profiles of the magnitudes of the total optical force are nearly the same, as shown in Figs. 4(a) and 4(b). However, the two situations correspond, respectively, to trapping and detraping extremes. This is illustrated through a detailed analysis of the optical potential energy landscape in Figs. 5(a) and 5(b). The optical potential energy ϕ , in units of $\varepsilon_0 E_0^2/k$, is derived from the gradient force in Eqs. (3) and (4). As shown in both cases, the gradient force is overwhelmingly dominant over the scattering force. The optical potential energy ϕ , however, shows a change from a periodic distribution of pits to that of humps, serving as a comprehensive picture for the trapping to detraping transition induced by the polarization.

In Figs. 5(c) and 5(d) we present the optical potential energy for the case corresponding to Figs. 2(c) and 2(d), in the case of a gold particle immersed in the three-beam optical lattice with different polarization. Although in both cases the scattering force is comparable to the gradient force, the potential energy derived from the latter still provides a vivid picture for the detraping to trapping transition. For the polarization $(p, q) = (1, 0)$, namely, with the electric field polarized along z to avoid the vectorial feature of the electromagnetic field, the potential energy landscape shows a periodic distribution of protuberances [see Fig. 5(c)], ruining any possible trapping since the scattering force will never construct a trap. On the other hand, when the polarization switches to $(p, q) = (0, 1)$, with the electric field polarized normal to z and the vectorial character coming into play, we see a dispersion of depressions in the potential energy landscape [see Fig. 5(d)], which, when tuned to surpass the scattering force, will leave us with a stable trapping, as shown in Fig. 2(d) in the radial force landscape, providing a typical example of achieving stable optical trapping by the effect due to polarization.

III. CONCLUSION

In this paper we studied the polarization effect on the spatial pattern of optical force acting on a particle immersed in a simple three-beam optical lattice, determined by Eqs. (1) and (2). A diversity of optical force landscapes was visualized due to the change of polarization, implying tunability of optical manipulation in optical lattice by simply modulating the polarization of optical beam, which results from the vectorial property of optical field. We then traced the underlying physical origin of the polarization effect in this three-beam optical lattice to the relative magnitude of the two essentially different types of optical force, namely, the conservative and nonconservative forces. In addition, we also presented genuine optical potential energy landscapes for optical lattices with different polarizations. The potential energy landscapes, either in the case where the conservative optical force is overwhelmingly dominant over the nonconservative force or in the case where the latter is comparable to the former, provide a comprehensive picture to understand the trapping and detraping transition induced by the polarization. Our results may shed some light on the understanding of light-matter interaction, as well as suggesting an alternative way to

tune the optical micromanipulation by changing polarization, taking full advantage of the vectorial property of the optical field.

ACKNOWLEDGMENT

This work was supported by the National Natural Science Foundation of China (Grant No. 11574055).

-
- [1] J. C. Maxwell, *A Treatise on Electricity and Magnetism*, 1st ed. (Oxford University Press, Oxford, 1873).
- [2] A. Ashkin, Acceleration and Trapping of Particles by Radiation Pressure, *Phys. Rev. Lett.* **24**, 156 (1970).
- [3] A. Ashkin, J. M. Dziedzic, J. E. Bjorkholm, and S. Chu, Observation of a single-beam gradient force optical trap for dielectric particles, *Opt. Lett.* **11**, 288 (1986).
- [4] A. Ashkin and J. Dziedzic, Optical trapping and manipulation of viruses and bacteria, *Science* **235**, 1517 (1987).
- [5] O. M. Maragò, P. H. Jones, P. G. Gucciardi, G. Volpe, and A. C. Ferrari, Optical trapping and manipulation of nanostructures, *Nat. Nanotechnol.* **8**, 807 (2013).
- [6] A. Ashkin, Optical trapping and manipulation of neutral particles using lasers, *Proc. Natl. Acad. Sci. USA* **94**, 4853 (1997).
- [7] D. G. Grier, A revolution in optical manipulation, *Nature (London)* **424**, 810 (2003).
- [8] K. Dholakia and P. Reece, Optical micromanipulation takes hold, *Nano Today* **1**, 18 (2006).
- [9] D. McGloin and J. Reid, Forty years of optical manipulation, *Opt. Photon. News* **21**, 20 (2010).
- [10] F. M. Fazal and S. M. Block, Optical tweezers study life under tension, *Nat. Photonics* **5**, 318 (2011).
- [11] M.-C. Zhong, X.-B. Wei, J.-H. Zhou, Z.-Q. Wang, and Y.-M. Li, Trapping red blood cells in living animals using optical tweezers, *Nat. Commun.* **4**, 1768 (2013).
- [12] J. Chen, J. Ng, Z. Lin, and C. Chan, Optical pulling force, *Nat. Photonics* **5**, 531 (2011).
- [13] K. T. Gahagan and G. A. Swartzlander, Optical vortex trapping of particles, *Opt. Lett.* **21**, 827 (1996).
- [14] K. Svoboda and S. M. Block, Optical trapping of metallic Rayleigh particles, *Opt. Lett.* **19**, 930 (1994).
- [15] M. A. Taylor, M. Waleed, A. B. Stilgoe, H. Rubinsztein-Dunlop, and W. P. Bowen, Enhanced optical trapping via structured scattering, *Nat. Photonics* **9**, 669 (2015).
- [16] T. M. Grzegorzczak, B. A. Kemp, and J. A. Kong, Stable Optical Trapping Based on Optical Binding Forces, *Phys. Rev. Lett.* **96**, 113903 (2006).
- [17] P. F. Barker and M. N. Shneider, Optical microlinear accelerator for molecules and atoms, *Phys. Rev. A* **64**, 033408 (2001).
- [18] J. C. Ndukaife, A. V. Kildishev, A. G. A. Nnanna, V. M. Shalaev, S. T. Wereley, and A. Boltasseva, Long-range and rapid transport of individual nano-objects by a hybrid electrothermoplasmonic nanotweezer, *Nat. Nanotechnol.* **11**, 53 (2016).
- [19] D. B. Ruffner and D. G. Grier, Optical Conveyors: A Class of Active Tractor Beams, *Phys. Rev. Lett.* **109**, 163903 (2012).
- [20] J.-M. R. Fournier, M. M. Burns, and J. A. Golovchenko, Writing diffractive structures by optical trapping, *Proc. SPIE Int. Soc. Opt. Eng.* **2406**, 101 (1995).
- [21] A. Casaburi, G. Pesce, P. Zemánek, and A. Sasso, Two- and three-beam interferometric optical tweezers, *Opt. Commun.* **251**, 393 (2005).
- [22] E. Schonbrun, R. Piestun, P. Jordan, J. Cooper, K. D. Wulff, J. Courtial, and M. Padgett, 3D interferometric optical tweezers using a single spatial light modulator, *Opt. Express* **13**, 3777 (2005).
- [23] E. R. Dufresne, G. C. Spalding, M. T. Dearing, S. A. Sheets, and D. G. Grier, Computer-generated holographic optical tweezer arrays, *Rev. Sci. Instrum.* **72**, 1810 (2001).
- [24] M. Woerdemann, C. Alpmann, M. Esseling, and C. Denz, Advanced optical trapping by complex beam shaping, *Laser Photon. Rev.* **7**, 839 (2013).
- [25] T. V. Raziman and O. J. F. Martin, Universal trapping in a three-beam optical lattice, *Phys. Rev. A* **98**, 023420 (2018).
- [26] Y. Hou, Z. Wang, Y. Hu, D. Li, and R. Qiu, Capture and sorting of multiple cells by polarization-controlled three-beam interference, *J. Opt.* **18**, 035401 (2016).
- [27] Y. K. Jiang, J. Chen, J. Ng, and Z. F. Lin, Decomposition of optical force into conservative and nonconservative components, [arXiv:1604.05138](https://arxiv.org/abs/1604.05138).
- [28] H. X. Zheng, X. N. Yu, W. L. Lu, J. Ng, and Z. F. Lin, Gcforce: Decomposition of optical force into gradient and scattering parts, *Comput. Phys. Commun.* **237**, 188 (2019).
- [29] J. D. Jackson, *Classical Electrodynamics*, 3rd ed. (Wiley, New York, 1999).
- [30] J. Ng, Z. F. Lin, C. T. Chan, and P. Sheng, Photonic clusters formed by dielectric microspheres: Numerical simulations, *Phys. Rev. B* **72**, 085130 (2005).
- [31] Q. Ye and H. Z. Lin, On deriving the Maxwell stress tensor method for calculating the optical force and torque on an object in harmonic electromagnetic fields, *Eur. J. Phys.* **38**, 045202 (2017).
- [32] G. Gouesbet and G. Gréhan, *Generalized Lorenz-Mie Theories*, 2nd ed. (Springer, Berlin, 2017).
- [33] P. B. Johnson and R. W. Christy, Optical constants of the noble metals, *Phys. Rev. B* **6**, 4370 (1972).
- [34] C. Oubre and P. Nordlander, Optical properties of metallo-dielectric nanostructures calculated using the finite difference time domain method, *J. Phys. Chem. B* **108**, 17740 (2004).
- [35] Y. Jiang, H. Lin, X. Li, J. Chen, and J. Ng, Hidden symmetry and invariance in optical force (unpublished).
- [36] S. Sukhov and A. Dogariu, Non-conservative optical forces, *Rep. Prog. Phys.* **80**, 112001 (2017).
- [37] C. F. Bohren and D. R. Huffman, *Absorption and Scattering of Light by Small Particles* (Wiley, New York, 1983).
- [38] A. Ashkin and J. P. Gordon, Stability of radiation-pressure particle traps: An optical Earnshaw theorem, *Opt. Lett.* **8**, 511 (1983).
- [39] K. C. Neuman and S. M. Block, Optical trapping, *Rev. Sci. Instrum.* **75**, 2787 (2004).